Chávez-Lara, C. M., Holtvoeth, J., Roy, P. D., & Pancost, R. D. (2018). A 27cal ka biomarker-based record of ecosystem changes from lacustrine sediments of the Chihuahua Desert of Mexico. *Quaternary Science Reviews*, *191*, 132-143. https://doi.org/10.1016/j.quascirev.2018.05.013

A 27cal ka biomarker-based record of ecosystem changes from lacustrine sediments of the Chihuahua Desert of Mexico

C.M. Chávez-Lara [a], J. Holtvoeth [a], P.D. Roy [b], R.D. Pancost [a]

[a]*Organic Geochemistry Unit, School of Chemistry, School of Earth Sciences, University of Bristol Cabot Institute, University of Bristol, Bristol, UK*

[b]*Instituto de Geología, Universidad Nacional Autónoma de México, Ciudad Universitaria, CP 04510, Ciudad de México, México*

Abstract

Hydroclimate variation of the northwest Mexico during the late Pleistocene and Holocene is an active area of debate, with uncertainty in the nature and sources of precipitation. Previous research has inferred the influences of winter storms, summer monsoonal rain and autumn tropical cyclones. The impacts on regional and local ecosystems, however, are not well constrained. Here, we investigate the response of lacustrine and terrestrial habitats of the Santiaguillo Basin in the Chihuahua Desert (Mexico) to hydrological changes occurring since the late last glacial. Biomarkers from the sediments reflect variable input of organic matter (OM) from algal and bacterial biomass, aquatic microfauna and surrounding vegetation, revealing distinct stages of ecosystem adaption over the last 27 cal ka. Based on previously published and new data, we show that a perennial productive lake was present during the late glacial and it persisted until 17.5 cal ka BP. Coinciding with Heinrich event 1, OM supply from deteriorating wetland soils may have been caused by early dry conditions. Further phases of increasing aridity and a shrinking water body drove changing OM quality and biomarker composition during the early and mid-Holocene. A pronounced shift in biomarker distributions at 4 cal ka BP suggests that the supply of plant litter from resinous trees and grasses increased, likely reflecting the establishment of modern vegetation. Our results illustrate the potential of biomarker applications in the area, adding to the evidence of hydroclimate variability and enabling reconstructions of local ecosystem dynamics.

Keywords: Organic Geochemistry; Continental Biomarkers; North America; Paleoclimatology; Paleolimnology; Pleistocene; Holocene

1. Introduction

The Chihuahua Desert is located between 22-32º N and 100-109º W and is the largest desert in North America. Its area of ~ 450,000 km^2 extends through the northern Mexican states of Chihuahua, Durango, Zacatecas, Nuevo Leon and San Luis Potosi and the southern USA states of New Mexico, Texas and Arizona (Palacios-Fest *et al*., 2002). Reconstructions of past climate variations in this desert have received significant attention over the last few decades, particularly with respect to the North American Monsoon (NAM) during the Late Quaternary. Previous records include lacustrine sediments, aeolian deposits, packrat middens and speleothems, producing proxy data through the distributions of pollen, diatoms and ostracods, inorganic geochemistry (X ray fluorescence, X ray diffraction, magnetic susceptibility) and stable isotopes (e.g. Lozano-García *et al*., 2002; Metcalfe *et al*., 2002; Roy *et al*., 2012, 2013, 2016; Chávez-Lara *et al*., 2015; Quiroz-Jimenez *et al*, 2017). These records have provided insight into past climatic change but the carbon cycling and vegetation responses to those changes are still poorly understood (Metcalfe *et al*., 2015).

Recent publications have presented different hypotheses with regard to the role of the NAM, winter storms and tropical cyclones in regional precipitation patterns during the last glacial maximum (LGM). Oster *et al*. (2015) argued that the location and strength of the contemporary pressure system were responsible for a higher contribution of winter precipitation from the Pacific Ocean to the southwestern USA during the LGM. In Northwest Mexico, however, the NAM was weaker during the LGM due to high latitude cooling that shifted the westerlies south, causing changes in the main wind direction and cold and dry conditions in the region (Bhattacharya *et al*., 2017). Furthermore, Roy *et al*. (2015) observed humid conditions in the Santiaguillo Basin in central northern Mexico during the LGM but concluded that, although the NAM was inactive or weaker, the frequent formation of tropical cyclones in the eastern North Pacific brought more albeit regionally restricted autumn rainfall. By contrast, based on speleothem record from tropical Southwest Mexico, Lachniet *et al*. (2013) argued that the NAM was active and attributed this to an active but shallow Atlantic Meridional Overturning Circulation and the proximity of their study site to the northern limits of the Intertropical Convergence Zone (ITCZ). Although the exact causes of climatic change in the Chihuahua Desert thus remain uncertain, it is still

useful to explore how those changes impacted local ecosystems. The development of the vegetation, for example, can also reflect changes in the seasonality of rainfall and, hence, may provide clues towards changes in the moisture source since the LGM. For the late glacial, pollen records indicate the presence of cold climate species, in contrast to the current dominance of desert shrublands in the southwestern USA (Van Devender, 1990; McAuliffe and Van Devender, 1998; Holmgren *et al*., 2003, 2006). Similarly, close to the Mexican border, packrat middens indicate the presence of summer-flowering annuals and the absence or minimal proportions of desert shrublands (Holmgren *et al*., 2007). During the early Holocene, the belt of greater winter precipitation shifted north. Associated with this was a migration of cold weather vegetation to higher latitudes and elevations over 2,000 m a.s.l., being replaced by shrub and desert species during the establishment of the North American deserts (Van Devender, 1990; Holmgren *et al*., 2003). For the mid to late Holocene, as the conditions became drier in northwestern Mexico, paleovegetation records become scarce due to fossil pollen being poorly preserved and sediments becoming organic lean, leaving unclear much of the overall biome development from the last glacial to today (e.g. Lozano-García *et al*., 2002; Metcalfe *et al*., 2002).

Lipid biomarkers in lacustrine sediments can be used to fill this gap (Meyers, 2003). The organic matter (OM) of lacustrine sediments is derived from the particulate detritus of aquatic plants and algae as well as vegetation present in the surrounding lake catchment. It contains a range of biomarkers that represent input of OM from different sources and subsequent diagenetic alteration (Perry *et al*., 1979). Both of these characteristics can be used to reconstruct environmental changes in ancient ecosystems (Meyers and Benson, 1988). In this paper, we present the lipid biomarkers in organic-poor sediments (total organic carbon concentration/TOC: 0.2-1.2%) deposited over the last 27 cal ka in the Santiaguillo Basin of central-northern Mexico. This is the first biomarker-based investigation of late Quaternary lacustrine sediments from Mexico, and we use these data to identify changes in the sources of organic carbon to the lake system during the late Pleistocene and Holocene, with implications for carbon cycling, and to reconstruct the paleovegetation of the Chihuahua Desert of Mexico.

2. Regional Setting

The Santiaguillo Basin is located in central-north Mexico (Figure 1), in the rain shadow of the Sierra Madre Occidental hills. It has an area of 1,964 km^2 within 24°30' to 25°00' N and from 104°40' to 105°00' W. Tectonic movements formed this basin during the Cenozoic, and its bedrock is composed of Cretaceous to Quaternary metamorphic, igneous, and sedimentary rocks (Nieto-Samaniego *et al*., 2012). The most recent deposits are lacustrine sediments and Quaternary alluvium (Nieto-Samaniego *et al*., 2012). A nearby meteorological station (Guatimape: 24°48'25" N, 104°55'19" W) provides mean monthly temperature and precipitation data from 1981 to 2010 AD (Source: Servicio Meteorologico Nacional, Mexico). The basin receives around 394 mm of its average annual precipitation of 445 mm between June and October and the rest of the year contribute around 51 mm of precipitation (Figure 1).

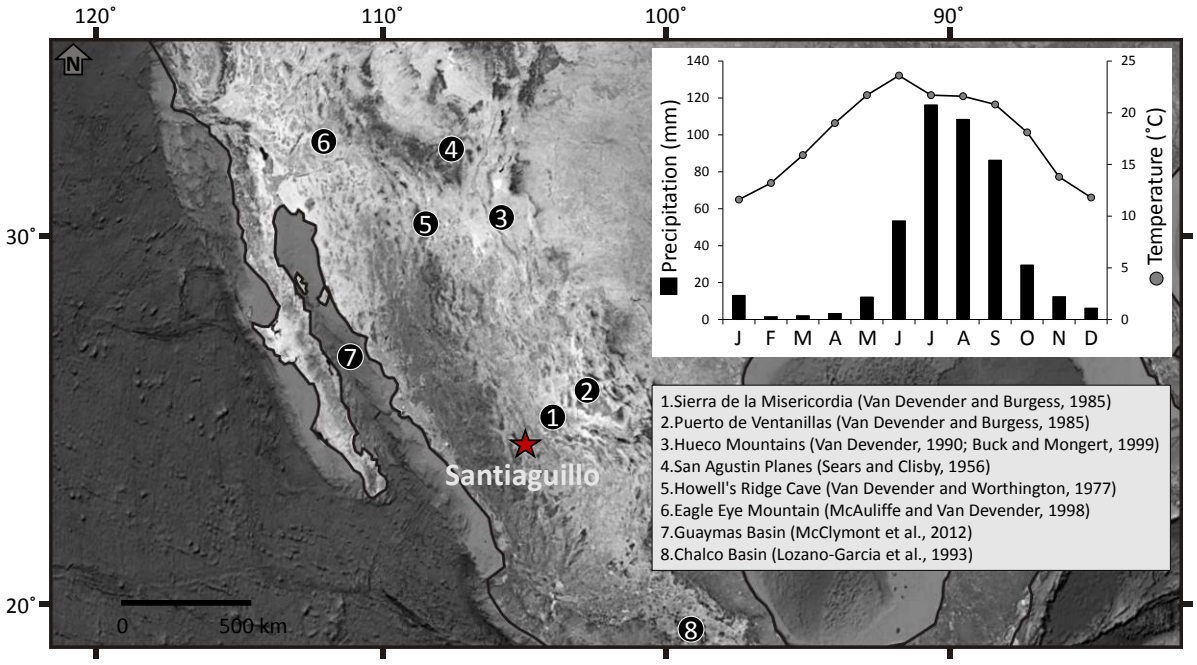

Figure 1 The Santiaguillo Basin (red star) is located in the central-northern Mexico. Location of other records used here for comparison (circles). Mean monthly temperature and precipitation from 1981 to 2010 AD are calculated from data obtained from the nearest meteorological station at Guatimape.

3. Materials and Methodology

Sediments were collected from a 3 m deep pit at the western border (24° 44′ N, 104° 48′ W, 1960 m a.s.l.) of the Santiaguillo Basin. The sedimentary record was divided in 2 cm intervals and stored in the Paleoenvironment and Paleoclimatology Lab at the Institute of Geology of the National Autonomous

University of Mexico. This sequence was previously studied for ostracod paleoecology, TOC contents, TOC/TN ratios (Chávez-Lara *et al*., 2015) and inorganic geochemistry (Roy *et al*., 2015) in order to reconstruct paleosalinity of the water column and the paleohydrological conditions of the basin. The stratigraphy of the sediment profile is from Roy *et al*. (2015): clay and calcareous silt represent the bottom 22 cm (300-278 cm depth), overlain by silty-clay (278-265 cm depth); intercalations of silty-sand and silt occur from 265 to 60 cm depths, and vertical desiccation fissures (~65 cm long) are preserved in sediments at 75 cm depth; on top of this large block of intercalations is a 10 cm layer of silty-clay (60-50 cm depth), and the upper 50 cm are composed of darker massive silty-sand with abundant root remnants. Occasional carbonate nodules are present from the bottom of the record to 75 cm depth. The chronology of the sequence is based on 7 radiocarbon (AMS) dates of organic carbon present in the bulk sediment (Table 1), and we have improved the previously presented age model (Roy *et al*., 2015) by including another radiocarbon date at 11 cm depth. Since all of the surrounding rocks are of igneous or metamorphic origin and are carbonate-free, we can rule out significant contributions of fossil/dead organic carbon and (old) dissolved inorganic carbon from the catchment and incorporation into the lacustrine biomass. We cannot exclude supply of pre-aged terrestrial organic carbon from soils in the catchment but synchronous responses of speleothems of southwest Mexico (Uranium–thorium dating; Lachniet *et al*., 2013) and the paleohydrology of the Santiaguillo Basin suggests that this effect might be minimal. Dates were calibrated by the online software Calib, version 7.0.2 (Reimer *et al*., 2013), within the 2σ interval and using the date of the highest probability. Accordingly, the sediment record represents the last 27,000 cal. years (27 cal ka; Figure 2) and sedimentation rates are relatively invariant at the resolution measured, between 0.01 to 0.013 cm year^{-1}.

Table 1 Radiocarbon dates of bulk sediment samples from different depths of the sedimentary record, Santiaguillo Basin. *Calib 7.0.2

Lab. code	**Depth** (cm)	**AMS ^{14}C age** (BP)	***Modeled calibrated age** (2σ, cal yr BP)	***Probability** (%)	***Age of highest prob.** (cal yr BP)
ICA15OS/0506	11	1,100±40	929-1085	98	979
Beta-299072	49	3,610±30	3838-3984	99	3,905
Beta-299073	73	5,250±30	5925-6030	67	5,980
Beta-321663	111	8,900±40	9897-10189	100	10,043
Beta-299074	167	13,360±60	15854-16267	100	16,082
Beta-299075	205	14,610±60	17603-17976	100	17,807
Beta-299076	279	20,790±100	24622-25391	100	25,110

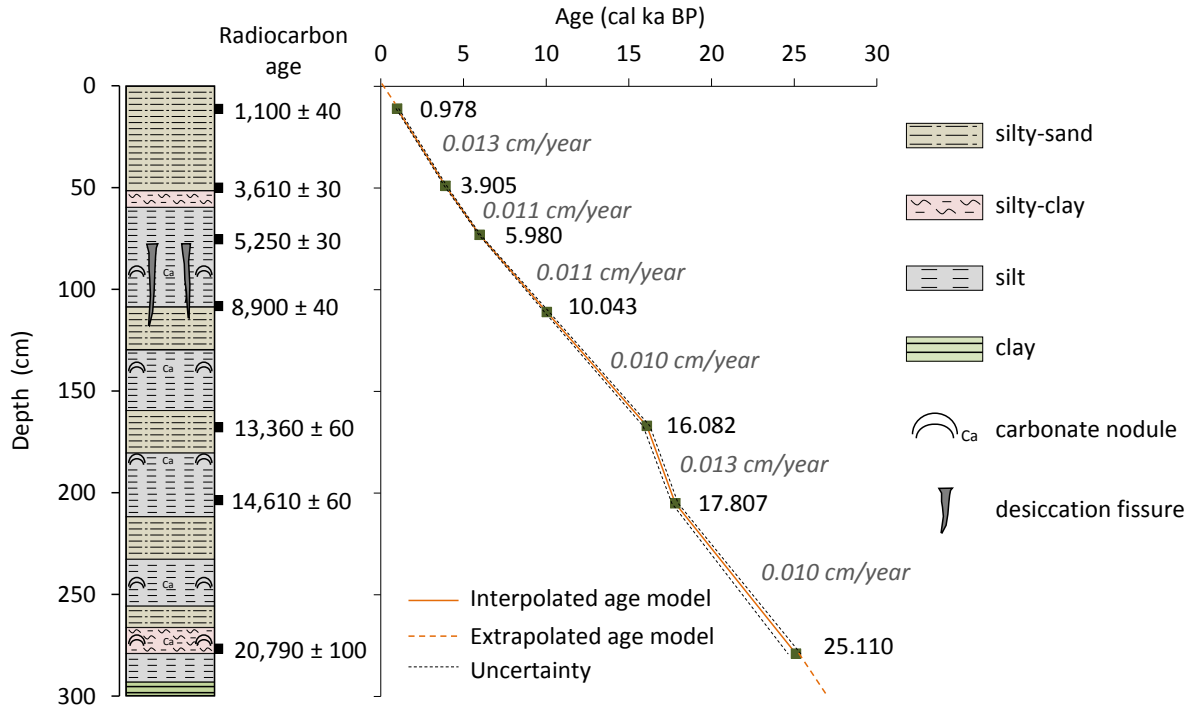

Figure 2 Stratigraphy of the sedimentary record and radiocarbon dates at different depths (black boxes). The age model is constructed using the calibrated values and suggests that sediments from the Santiaguillo Basin represent the depositional history of the last 27,000 cal. years.

All samples were freeze-dried and homogenized with mortar and pestle. The powdered sediment from a subset of 31 samples was weighed and transferred to a clean glass culture tube. 5α-cholestane was added to each sediment sample, with the amount of internal standard adjusted for the concentration of total organic carbon (TOC) previously reported by Chávez-Lara *et al*. (2015). The sediment samples were extracted using a microwave-assisted extraction system (EthosEX, fitted with temperature control and glass liners in self-venting extraction vessels), with a solvent mix of dichloromethane and methanol (9:1) at 70°C for 20 minutes. In order to completely remove any residual water, the resulting total lipid extracts (TLEs) were eluted over sodium sulphate columns.

In order to transmethylate fatty acids, i.e. converting them into GC-amendable methyl esters, about 1 mL of acetyl chloride-methanol (1:30) was added to an aliquot of TLE. Samples were then heated at 45 °C for 12 h, and excess acetyl chloride-methanol was evaporated under a gentle flow of nitrogen. The extracts were then passed through potassium carbonate columns in order to remove excess acids. About 25 μL of N, O-bis(trimethylsilyl)trifluoroacetamide (BSTFA) were added to the transmethylated TLE, and samples were then heated at 65 °C for 1 h to convert alcohol moieties into TMS ethers. Excess BSTFA was evaporated under a gentle flow of nitrogen.

The derivatised lipid extracts were dissolved in DCM prior to GC/MS analysis. 1 μl was manually injected on the GC-MS. The equipment used was a Thermo Scientific Trace 1300 gas chromatograph fitted with a Restek RTX-1 fused silica column (dimethyl polysiloxane; 50 m x 0.32 mm x 0.17 μm), linked to a Thermo Scientific ISQ mass spectrometer operating with electron ionization at 70 eV and scanning a m/z range of 50-650. Helium was used as carrier gas. The temperature program was: 60 ºC initial temperature, held for 1 minute, before increasing to 170 ºC at 6 ºC min^{-1}, followed by an increase to 315 ºC at 2.5 ºC min^{-1}; the temperature was held at 315 ºC for 10 minutes. The acquisition and analysis of the MS data was carried out using XCalibur software. Compound identifications were assigned by comparing the mass spectra and relative retention times with those from the literature. Fatty acids (FAs) were determined as their derivatives - fatty acid methyl esters (FAMEs). Alcohols and sterols were determined as their trimethylsilyl derivatives. Quantification was based on the peak areas of the target compound versus that of the 5α-cholestane internal standard. This type of analysis is semi-

quantitative because it is likely that response factors differ among compound classes. Instead, we present their relative compositional changes to infer the ecosystem changes.

4. Results

4.1. Lipid concentrations

The total lipid concentration fluctuates between 0.4 and 34 μg/g_{sed} (Figure 3) with an average of 7.5 μg/g_{sed}. Higher concentrations (3.5-34 μg/g_{sed}) occur in sediments at the bottom of the record, from 299-201cm (27-17.6 cal ka BP), and in the uppermost 31 cm (last 2.5 cal ka). Abundances of individual lipids are presented as percentages of the sum of all quantified lipids (%$_{lipids}$).

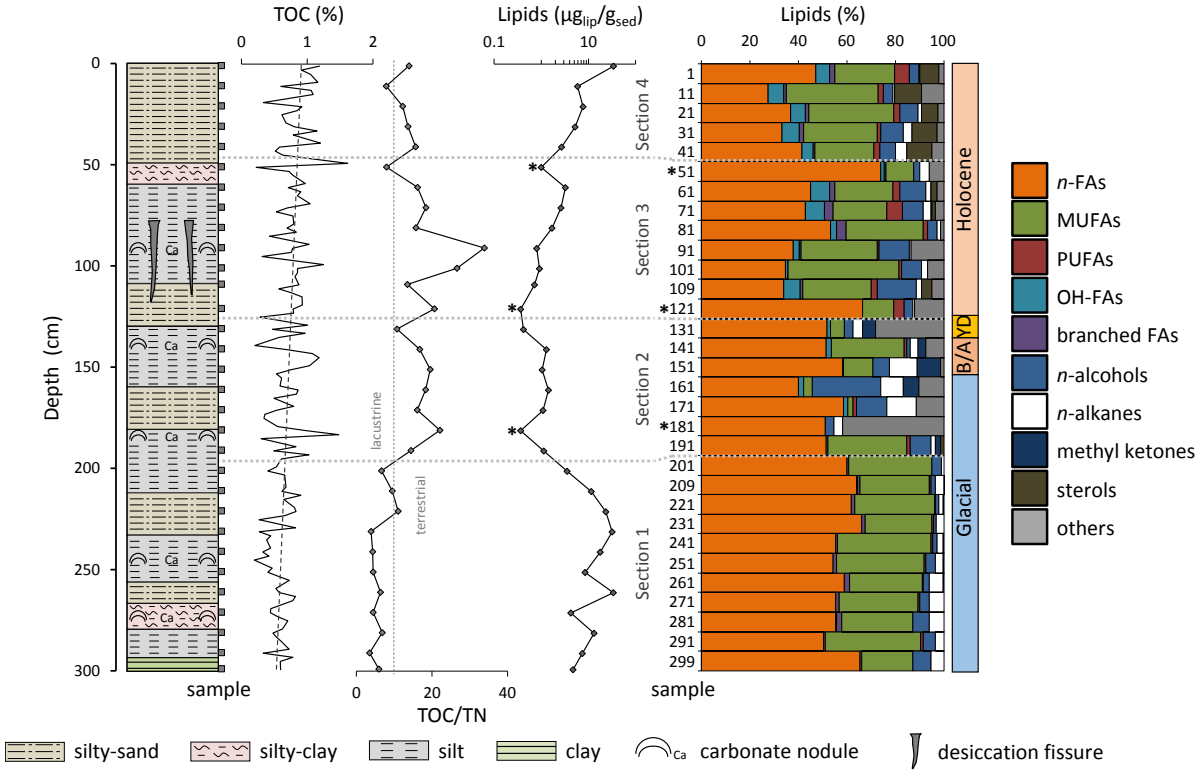

Figure 3 Stratigraphic profile of the sedimentary record and geochemical data from elemental (total organic carbon: TOC, in weight%; total organic carbon to total nitrogen ratio: TOC/TN) and biomarker analyses (lipid concentration in μg per g sediment; lipid composition: bar diagram), with sample distributions (gray boxes) over depth. The elemental data (TOC, TOC/TN) are taken from Chávez-Lara *et al*. (2015). Note that he total lipid concentration (μg/g_{sed}) is presented on logarithmic scale. The record is divided into four sections based on geochemical characteristics and biomarker distributions as

described in section 5. The asterisk (*) marks sediments with highly anomalous lipid compositions resulting from very low lipid concentrations, leaving many compounds below the detection limit. These samples have not been considered for further interpretation.

4.2. Lipid composition (compound class inventory)

We quantified saturated *n*-fatty acids, mono- and poly-unsaturated fatty acids, hydroxy fatty acids, branched fatty acids, *n*-alcohols, *n*-alkanes, methyl ketones, sterols, and a range of miscellaneous compounds, mainly β-amyrin, α-amyrin and methoxy acids (Figure 3, summary in Table 2, for complete compound list see supplement). In general, these include the vast majority of GC-amenable compounds in the TLEs. Glycerol dialkyl glycerol tetraethers (GDGTs) were present but in abundances too low for quantification.

Table 2 Summary of the quantified compound classes found in 31 sediment samples collected from the Santiaguillo sedimentary record. The concentrations are expressed as $\%_{lipids}$. (*sediments with extremely low lipid concentrations and resulting anomalous composition, ignored for further interpretation)

Depth (cm)	Age (cal ka BP)	total *n*-FAs	short *n*-FA	mid *n*-FA	long n-FA	OH-FAs	α-OH-FAs	ω-OH-FAs	branched FAs	MUFAs	PUFAs	OHs	*n*-alkanes	methyl ketones	sterols	others
1	0.1	47.1	19.8	16.5	10.8	5.8	1.0	4.6	2.3	24.5	6.3	3.9	0.4	-	7.6	2.2
11	1.0	27.4	17.3	6.4	3.8	6.5	5.5	1.0	0.9	38.2	2.1	3.9	0.7	-	11.2	9.0
21	1.8	36.9	16.1	6.1	14.8	6.0	2.0	4.0	1.4	35.1	2.3	7.5	1.6	-	6.8	2.2
31	2.5	33.4	12.0	5.5	15.9	7.1	2.1	4.6	1.8	30.3	1.4	9.2	3.6	-	10.4	2.9
41	3.3	41.4	19.1	11.0	11.2	4.9	3.1	1.8	0.5	24.3	2.6	6.4	4.8	-	10.4	4.9
*51	4.1	74.1	24.0	21.8	28.3	1.4	1.4	-	0.5	11.4	-	2.6	4.2	-	-	5.8
61	4.9	45.0	23.7	7.5	13.9	8.1	5.1	-	2.1	23.9	2.8	10.9	1.8	-	2.6	2.7
71	5.8	42.8	30.2	7.7	4.9	8.2	6.1	1.4	3.4	22.2	6.3	8.6	3.5	0.1	1.6	3.4
81	6.8	53.3	39.8	9.7	3.8	2.4	2.4	-	3.8	31.8	1.9	3.8	1.4	-	-	1.5
91	7.9	37.9	9.6	16.8	11.4	2.7	2.3	0.4	0.4	31.6	0.8	12.2	0.8	-	-	13.6
101	9.0	34.8	12.1	9.9	12.9	0.8	0.8	-	0.3	45.7	0.9	8.2	2.5	-	-	6.8
109	10.0	33.8	16.3	12.3	5.3	7.1	5.4	1.6	1.0	28.0	2.5	16.2	2.3	-	4.2	4.8
*121	11.1	66.4	36.9	21.7	7.8	-	-	-	-	13.0	4.1	3.8	0.7	-	-	11.9
131	12.2	51.8	15.1	22.0	14.7	1.5	1.5	-	-	5.7	-	3.3	4.0	5.4	-	28.2
141	13.3	51.5	14.1	11.6	25.9	2.0	1.7	0.3	-	30.1	1.2	1.2	3.2	3.4	-	7.4
151	14.4	58.4	3.7	17.7	37.0	0.3	0.3	-	-	12.0	-	6.8	11.7	9.6	-	1.2
161	15.4	40.1	3.7	16.3	20.2	2.2	0.2	2.0	-	3.6	-	28.0	9.3	6.5	-	10.3
171	16.3	58.7	16.2	14.9	27.7	1.6	1.1	0.5	-	2.3	1.1	12.7	12.2	-	-	11.3
*181	16.7	51.0	27.0	10.4	13.6	-	-	-	-	-	-	3.7	3.7	-	-	41.7
191	17.2	51.4	17.7	15.8	17.9	0.8	0.8	-	-	32.6	1.2	8.7	1.7	2.2	1.3	-
201	17.6	60.2	55.8	3.4	1.0	-	-	-	0.8	34.3	-	3.7	1.0	-	-	-
211	18.4	64.0	62.7	1.2	0.1	0.2	0.2	-	1.3	28.5	0.7	1.8	3.4	-	-	-
221	19.4	61.8	60.2	1.2	0.4	-	-	-	1.4	33.0	0.4	1.4	1.8	0.1	-	-
231	20.4	66.2	65.4	0.6	0.2	-	-	-	1.3	27.7	0.6	1.2	3.0	-	-	-
241	21.4	55.4	50.9	2.6	1.9	-	-	-	0.9	38.5	0.7	1.6	2.6	0.3	-	-
251	22.4	54.2	49.8	2.4	2.0	-	-	-	1.5	36.2	0.6	4.0	3.4	0.1	-	-
261	23.3	58.9	57.4	1.2	0.4	0.1	-	0.1	2.2	29.7	0.6	2.5	5.7	0.2	-	-
271	24.3	55.4	51.5	3.1	0.9	-	-	-	1.4	32.4	1.0	3.8	6.0	-	-	-
281	25.3	55.3	49.5	2.6	3.1	0.5	0.5	-	2.1	29.3	-	6.9	6.0	-	-	-
291	26.3	50.5	43.4	4.5	2.6	-	-	-	0.7	39.4	0.8	5.0	3.5	-	-	-
299	27.1	65.3	56.8	3.8	4.8	-	-	-	1.0	21.1	-	7.4	5.3	-	-	-

185 *4.2.1. Saturated n-fatty acids (n-FAs)*

186 Saturated *n*-fatty acids (*n*-FAs) represent the major lipid group, with the summed abundance fluctuating
187 between 27 to 74 $\%_{lipids}$ (average 51 $\%_{lipids}$). Higher proportional abundances (> average) occur in the
188 deepest sediments, from 299-201 cm (27-17.6 cal ka BP), although discrete sediment horizons at depths
189 of 121 cm (11.1 cal ka BP) and 51 cm (4.1 cal ka BP) have abundances of 66 $\%_{lipids}$ and 74 $\%_{lipids}$
190 respectively.

191 *4.2.2. Mono- and polyunsaturated fatty acids (MUFAs and PUFAs)*

192 Monounsaturated FAs (MUFAs) comprise the second major lipid group, and relative abundances
193 fluctuate between 2 and 46 $\%_{lipids}$ (average 26 $\%_{lipids}$). Higher abundances (> average) typically occur in
194 the deepest sediments, from 299-191 cm (27-17.2 cal ka BP), and in the top 109 cm (last 10 cal ka).
195 Only the sediment at 181 cm depth (16.7 cal ka BP) contained no detectable MUFAs. Polyunsaturated
196 FA (PUFAs) proportional abundances are < 6.3 $\%_{lipids}$ (average 1.4 $\%_{lipids}$). Higher abundances (>
197 average) occur in sediments from the upper 121 cm depths (last 11.1 cal ka).

198 *4.2.3. Hydroxy acids (OH-FAs)*

199 Hydroxy fatty acid (OH-FAs) relative abundances are < 8.2 $\%_{lipids}$ (average 2.3 $\%_{lipids}$). Higher
200 abundances (> average) occur in sediments from the upper 109 cm depths (last 10 cal ka).

201 *4.2.4. Branched fatty acids*

202 Branched FA relative abundances – mainly *iso*- and *anteiso*- C_{15}, *iso*-C_{16} and *iso*- and *anteiso*- C_{17}
203 components – are < 3.8 $\%_{lipids}$ (average 1.1 $\%_{lipids}$). Higher abundances (> average) occur in the deepest
204 sediments, from 299-211 cm (27-18.4 cal ka BP), and in the upper 81 cm (last 6.8 cal ka).

205 *4.2.5. n-Alkanes*

206 *n*-Alkane relative abundances fluctuate between 0.4 and 12 $\%_{lipids}$ (average 3.7 $\%_{lipids}$). Higher
207 abundances (> average) typically occur in the lower half of the core, from 299-131 cm (27-12.2 cal ka

208 BP), and in sediments from the upper 51 cm (last 4.1 cal ka). Distributions of n-alkanes differ
209 significantly (Figures 4 and 5) and are interpreted below.

210 *4.2.6. n-Alcohols (OH)*

211 *n*-Alcohol (OH) relative abundances fluctuate between 1.2 to 28 $\%_{lipids}$ (average 3.7 $\%_{lipids}$). Higher
212 abundances (> average) occur in most of the sediments but particularly high abundances (10 to 28
213 $\%_{lipids}$) occur in sediments at 171 cm (16.3 cal ka BP), 161 cm (15.4 cal ka BP), 109 cm (10 cal ka BP),
214 91 cm (7.9 cal ka BP) and 61 cm (4.9 cal ka BP).

215 *4.2.7. Methyl ketones*

216 Methyl ketone relative abundances are < 10 $\%_{lipids}$ (average 1.1 $\%_{lipids}$). Higher contents (> average)
217 occur in sediments at 191 cm depth (17.2 cal ka BP) and from depths of 161-131 cm (15.4-12.2 cal ka
218 BP).

219 *4.2.8. Sterols*

220 Sterol relative abundances – mainly sitosterol, stigmasterol and campesterol – are < 11 $\%_{lipids}$ (average
221 1.8 $\%_{lipids}$). Higher abundances (> average) occur at 191 cm (17.2 cal ka BP), 109 cm (10 cal ka BP)
222 and in the upper 71 cm of the profile (last 5.8 cal ka).

223 *4.2.9. Others*

224 Other identified compounds include β-amyrin (< 11 $\%_{lipids}$, average 1.6 $\%_{lipids}$), α-amyrin (< 1.6 $\%_{lipids}$,
225 average 0.1 $\%_{lipids}$) and 13-methoxyheneicosanoic acid (< 42 $\%_{lipids}$, average 3 $\%_{lipids}$). They occur only
226 in sediments between 181 and 0 cm (last 16.7 cal ka). Sediments at 181 cm depth (16.7 cal ka BP)
227 contain a particularly high relative abundance (42 $\%_{lipids}$) of 13-methoxyheneicosanoic acid.

228 **5. Discussion**

229 *5.1. Degradation*

We did not observe any correlation of lipid concentrations with previously published TOC contents (Chávez-Lara *et al*., 2015), and there is no indication of a significant down-core degradation of lipids. Moreover, the summed lipid abundances vary by at least an order of magnitude more than TOC contents (Figure 3). This suggests that a persistent background of reworked lipid-poor organic matter dominates the litter and changes in lipid concentrations reflect the more dynamic organic pool, including ecosystem and biogeochemical changes in source inputs. Although there does not appear to be downcore degradation of all lipids, it is possible that the reactive lipids (i.e. PUFAs and MUFAs) were preferentially degraded which would partially explain their high proportional abundances in the shallowest sediments; therefore, their profiles are interpreted cautiously. TOC/TN ratios do appear to vary with lipid concentrations, with low TOC/TN ratios corresponding to higher lipid concentrations and vice versa (Figure 3). Apart from the aquatic and terrestrial vegetation, it is likely that some of the TN in this organic-poor system was sourced from clay-associated ammonium (Freudenthal *et al*., 2001; Calvert., 2004), such that organic C/N ratios are likely higher.

Three sediments at 181 cm (16.7 ka cal BP), 121 cm (11.1 ka cal BP) and 51 cm (4.1 ka cal BP) depths have highly anomalous lipid compositions and very low lipid concentrations (Figure 3). They could have experienced particularly intense oxidative degradation. For example, the 181 cm sample is present at the lithological boundary between silty-clay and darker silty-sand and is associated with root remnants. It might have experienced a variety of episodic or transitory processes, including diagenetic changes (e.g. Meyers *et al*., 1984), associated with drying. Therefore, we avoided these three samples in our interpretations and focussed on generalised broader trends in lipid composition to evaluate environmental processes.

5.2. Inferred paleoenvironment from lipid assemblages

Based on the lipid assemblages and concentrations, the sediment sequence can be divided into four sections as described below and shown in Figures 4 and 5.

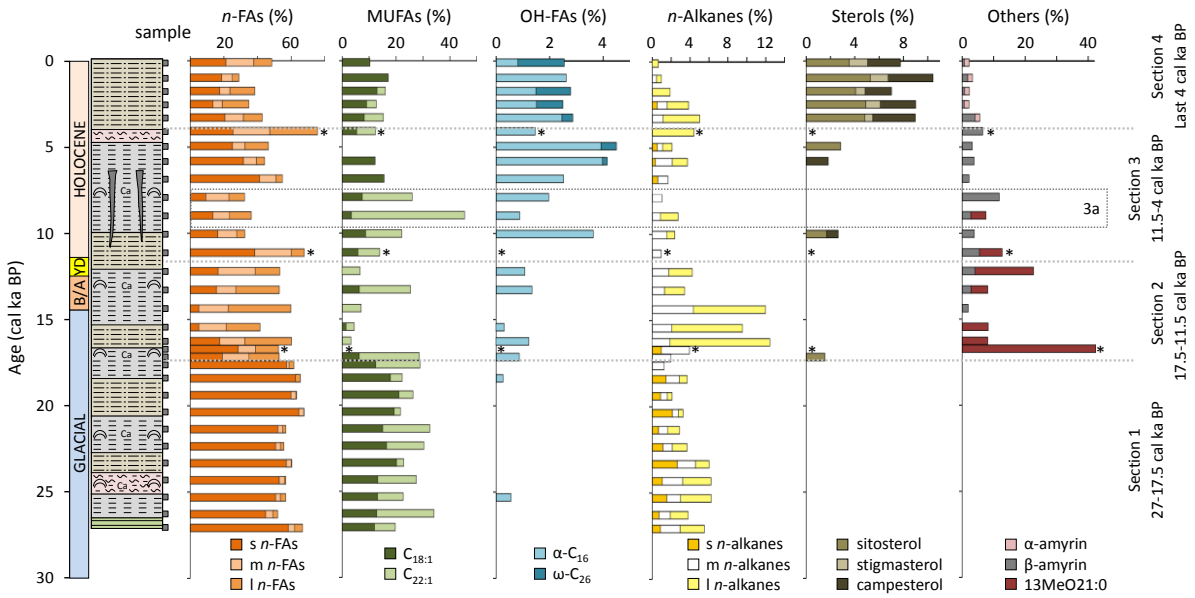

Figure 4 Stratigraphic profile of the sedimentary record (boxes on side of profile are sampled layers) compared to lipid biomarker distributions over time. Key compositional changes (%) of *n*-fatty acids (*n*-FAs), monounsaturated FAs (MUFAs), hydroxy acids (OH-FAs), *n*-alkanes, sterols and other compounds are shown, as well as sections defined in the text: Section 1 (27-17.5 cal ka BP), Section 2 (17.5-11.5 cal ka BP), Section 3 (11.5-4 cal ka BP) and Section 4 (last 4 cal ka). Section 3 has a subsection (3a). *Sediments with extremely low lipid concentrations and resulting anomalous composition, ignored for further interpretation.

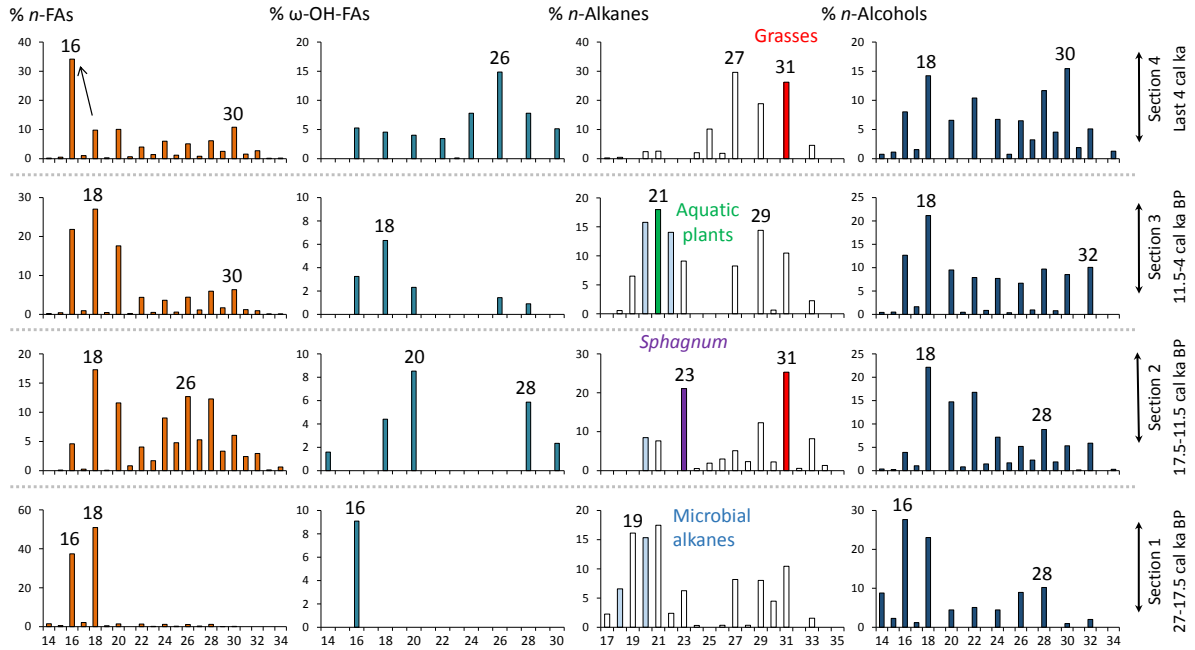

Figure 5 Averaged (by section) distributions, by chain length, of *n*-fatty acids, ω-hydroxy acids, *n*-alkanes and *n*-alcohols from section 1 (27-17.5 cal ka BP), section 2 (17.5-11.5 cal ka BP), section 3 (11.5-4 cal ka BP) and section 4 (last 4 cal ka BP). Average values (*y* axis) are percentages of the total amount of each compound class, i.e. $\%_{n\text{-FAs}}$, $\%_{\omega\text{-OH-FAs}}$, etc.

Section 1 (299-201 cm, 27-17.5 cal ka BP): Section 1 includes sediments at the bottom of the sequence and is characterized by high total lipid concentrations and higher proportions of short-chain fatty acids (s *n*-FAs) such as C_{16} and C_{18}. This is expressed in the ratio of short-chain C_{16} and C_{18} over the long chain C_{26} to C_{32} *n*-FA ($C_{16,18}/C_{26\text{-}32}$ FA, Fig. 6). These short-chain compounds are near ubiquitous in the environment, deriving from membrane lipids of all eukaryotes and most bacteria (Matsuda and Koyama, 1977), but also being part of biopolyesters such as cutin and suberin (Kolattukudy, 1981). In this section we inferred C_{16} and C_{18} *n*-FAs derive from phytoplankton and bacteria, based on the general geochemical fingerprint of the sediments that represent this interval. Short-chain *n*-FAs are dominated by C_{18} FA, which is rather unusual given that most algal FA is dominated by C_{16} (Brooks *et al*., 1976). We attribute high proportions of C_{18} *n*-FA to an increased contribution of bacterial biomass, consistent with a short chain *n*-alkane distribution ($C_{17\text{-}21}$) with high proportions of even-numbered *n*-alkanes. Section 1 also contains high proportions of C_{17} and C_{19} *n*-alkanes, generally considered as indicators of algae and photosynthetic bacteria (Han *et al*., 1968; Han and Calvin, 1969; Cranwell *et al*., 1987; Meyers, 2003). Typically, *n*-alkanes have odd carbon-number predominance (Debyser *et al*., 1975; Dastillung and Corbet, 1978), but in some settings even-numbered *n*-alkanes, especially the C_{14}-C_{22} homologues, occur in elevated proportions and have been attributed to a bacterial source (Grimalt *et al*., 1986; Grimalt and Albaigés, 1987). Similarly, the short chain OHs (primarily the C_{16} and C_{18} homologues) are mainly derived from phytoplankton and bacteria (Meyers and Ishiwatari, 1993). High proportions of $C_{18:1}$ MUFA also could derive from phytoplankton and bacteria (Bobbie and White, 1980; Kattner *et al*., 1983; Ahlgren *et al*., 1992). However, the near absence of hydroxy acids (OH-FAs) – except from small amounts of α- and ω-C_{16} OH-FA at 25.3 cal ka BP, 18.4 cal ka BP (α-) and 23.3 cal ka BP (ω-) – suggests a minimal relative contribution from bacterial biomass (Bobbie and White, 1980; Kattner *et al*., 1983; 273 Ahlgren *et al*., 1992). One possible explanation for the near

absence of OH-FAs and the lack of sterols is that cyanobacteria are the main lipid source in this section. However, these photosynthetic prokaryotes have higher proportions of C_{16} over C_{18} saturated *n*-FAs, as well as C_{16} over C_{18} MUFA (Cohen and Vonshak, 1991; Singh *et al*., 2002). Therefore, a cyanobacterial source of the LMW components remains equivocal. Overall, we suggest a mixed aquatic origin of organic matter that includes some significant bacterial contributions to specific compound classes. The absence of sterols, amyrins and methoxy acids, as well as low abundances of long-chain *n*-FAs, *n*-alkanes and *n*-OH, indicate minimal terrestrial vegetation input to the core site.

Section 2 (201-131 cm, 17.5-11.5 cal ka BP): Section 2 is characterised by significantly higher proportions of long-chain *n*-FAs, *n*-alkanes and *n*-OHs. This is expressed by a decrease in $C_{16,18}/C_{26-32}$ *n*-FA ratios and C_{16-24}/C_{25-34} *n*-alkane ratios (Fig. 6). Long-chain *n*-FAs, OHs and n-alkanes are derived nearly exclusively from leaf waxes of terrestrial plants (Eglinton and Hamilton, 1967; Řezanka and Sigler, 2009) (Maffei, 1996; Ficken *et al*., 2002). Between 16.3 and 14.4 ka, the proportion of *n*-alkanes was significantly higher (8.6 vs. 1.4 $\%_{lipids}$ on average of the entire record), with C_{31} being the dominant chain-length. This suggests input from a grassy environment since grasses contain higher amounts of *n*-alkanes as a proportion of the total lipids compared to leaf litter (Rommerskirchen *et al*., 2006; Cui *et al*., 2008; Holtvoeth *et al*., 2016; Bliedtner *et al*., 2017) and are frequently dominated by the C_{31} *n*-alkane, but we recognise the complexity of inferring sources of specific *n*-alkanes, especially in the absence of detailed reference plant analyses. Despite the long-chain *n*-alkane predominance, the distribution is bimodal with a high proportion of C_{23} *n*-alkane. Although *n*-alkanes are derived from a wide range of sources, some mid-chain *n*-alkanes can indicate input from more specific sources if present in a greater proportion, such is the case of C_{23} *n*-alkane which is abundant and frequently the dominant *n*-alkane in many *Sphagnum* species (Baas *et al*., 2000; Nott *et al*., 2000). The absence of α-amyrin but low amounts of β-amyrin could be indicative of minimal leaf, bark and resin inputs (Volkman, 2005; Hernández-Vázquez *et al*., 2012). The near absence of $C_{18:1}$ MUFA, and only small amounts of OH-FAs and short-chain *n*-alkanes (except at 16.7 cal ka BP) indicate low inputs from phytoplankton, bacteria or microalgae (Bobbie and White, 1980; Kattner *et al*., 1983; Ahlgren *et al*., 1992). This section is also characterised by the highest proportions of 13-methoxyheneicosanoic

(13MeO21:0), which is rare in lacustrine ecosystems. This methoxy acid has been identified in the red alga *Schizymenia dubyi* (Barnathan *et al*., 1998) in the Mediterranean and waters of Japan and Australia but has never been reported from lacustrine ecosystems (Ramirez *et al*., 2012). Kerger *et al*. (1986) identified a series of methoxy acids (10MeO18:0, 11MeO18:0, 12MeO20:0, 13MeO20:0) and interpreted them as biomarkers from sulphur bacteria (*Thiobacillus* spp.). This organism is halophilic and the optimal conditions for growing are in hypersaline lakes (Wood and Kelly, 1991). However, ostracod assemblages suggest that the Santiaguillo Basin hosted a lacustrine system with oligohaline to mesohaline water (Chávez-Lara *et al*., 2015). On the other hand, methoxy acids are also likely products from chemical alteration of FAs containing a cyclopropane unit (CFAs) during catalysed transmethylation (Orgambide *et al*., 1993). CFAs are major phospholipid components of many bacteria species (Grogan and Cronan, 1997) and appear to stabilize bacterial membranes under adverse conditions such as enhanced osmotic pressure or higher temperatures (Poger and Mark, 2015). It is thus reasonable to assume that the 13-methoxyheneicosanoic acid found in the Santiaguillo sediments were derived from a C_{22} CFA of bacterial origin, potentially growing under elevated salinity.

Section 3 (131-51 cm, 11.5-4 cal ka BP): This section largely coincides with the youngest silt layer and contains highly variable lipid distributions. It has lower proportions of mid- and long-chain *n*-FA compared to the under- and over-lying sections. This and other lipid biomarkers suggest a decrease in the contribution of terrestrial vegetation and an increase of bacterial and microalgal input (high proportions of short-chain *n*-FA and high relative abundance of even-numbered *n*-alkanes). Overall, this section shows high proportions of C_{21} *n*-alkane, likely indicative of aquatic plants (Cranwell, 1984), and contains the highest amounts of OH-FA in the sequence, with α-C_{16} OH-FA, likely sourced from bacteria (Yano *et al*., 1971), being the dominant compound.

Subsection 3a corresponds to an interval from 9 to 7.9 cal ka BP (101-91 cm), and it is characterised by a decrease in bacterial and microalgal input (low proportions of short-chain *n*-FAs, short- and mid-chain *n*-alkanes and α-C_{16} OH-FA), and the highest amounts of $C_{22:1}$ MUFA, which is a major compound produced by copepods to maximize the buoyancy effect of their wax esters (Arts *et al*., 2001). However, it also contains high amounts of β-amyrin (despite low leaf wax inputs), potentially indicating lower

leaf wax inputs but stronger bark and resin inputs. This subsection coincides with the highest TOC/TN ratios (> 20) from the record.

Section 4 (51-0 cm, last 4 cal ka BP): Section 4 is characterised by the highest proportions of sitosterol, campesterol and stigmasterol. Sterols occur in a range of sources, being present in all eukaryote organisms (Volkman, 1986); as such they derive from both algal and aquatic and higher plant inputs, with the latter typically associated with a dominance of C_{29} and sometimes C_{28} components, i.e. the Santiaguillo sterols are the three major sterols in higher plants (Goad and Goodwin, 1972). Moreover, this section is the only one from the Santiaguillo record that contains both α- and β-amyrin, continuing the trend from Section 3 of increasing higher plant bark and resin inputs. Particularly high amounts of α-amyrin have been found in the resins of *Bursera* and *Protium* species of the *Burseraceae* family (Hernández-Vázquez *et al*., 2012), which are common in the modern subtropical dry forest vegetation of the region (Porter, 1974; Espinosa *et al*, 2006). Diagenetically modified counterparts, i.e. *des*-A-triterpenoids (*des*-A-lupane, *des*-A-ursenes, *des*-A-oleanenes), reported from sediments of Lake Challa (East Africa; van Bree *et al*., 2016) were not detected here. Compared with the Section 3, Section 4 has higher proportions of long-chain *n*-alkanes that mainly peak at C_{27} and C_{31}, possible indicating higher inputs from woody angiosperms (dry forest vegetation) dominated by the C_{27} *n*-alkane and grasses dominated by the C_{31} *n*-alkane rather than two types of woody angiosperm species (e.g. Bush and McInerney, 2013). Higher proportions of long-chain ω-OH-FAs, mainly peaking at C_{26}, are also indicative of terrestrial plants. The ω-OH-FAs are major components of plant macromolecules such as cutin, and suberin (Baker and Martin, 1963; Kunst and Samuels, 2003; Samuels *et al*., 2008). A unique feature of this section is the shift in short-chain *n*-FAs dominance from C_{18} to C_{16} *n*-FA (Fig. 5).

5.3. Interpretation of Changing Ecosystems and Land Surface Processes

The hydroclimate of the Santiaguillo Basin and its catchment was controlled by dynamics of the North American Monsoon and tropical cyclones over the last 27 cal ka (Roy *et al*., 2015). Both regional and local factors would have influenced the development of the limnic ecosystem as well as the surrounding terrestrial habitats. The biomarker record shows four different sections that represent a combination of

biogeochemical, earth surface and ecosystem developments in response to changes in the local hydrological regime. In the following, we interpret the multi-proxy dataset with respect to ecosystem changes in chronological order and compare the results with previously published proxies such as a titanium (Ti)-based runoff record and TOC/TN ratios (Chávez-Lara *et al*., 2015; Roy *et al*., 2015; Figure 6). Previous regional (Figure 1) paleovegetation reconstructions from pollen archives (Sears and Clisby, 1956; Lozano-García *et al*., 1993), packrat middens (Van Devender, 1990; McAuliffe and Van Devender, 1998) and vertebrate fossils (Van Devender and Worthington, 1977) are used for comparison. For clarity in the discussion below, we divide the Holocene into early Holocene (11.7- 8.2 ka BP), mid Holocene (8.2-4.2 ka BP) and late Holocene (last 4.2 ka) after Walker *et al*. (2012).

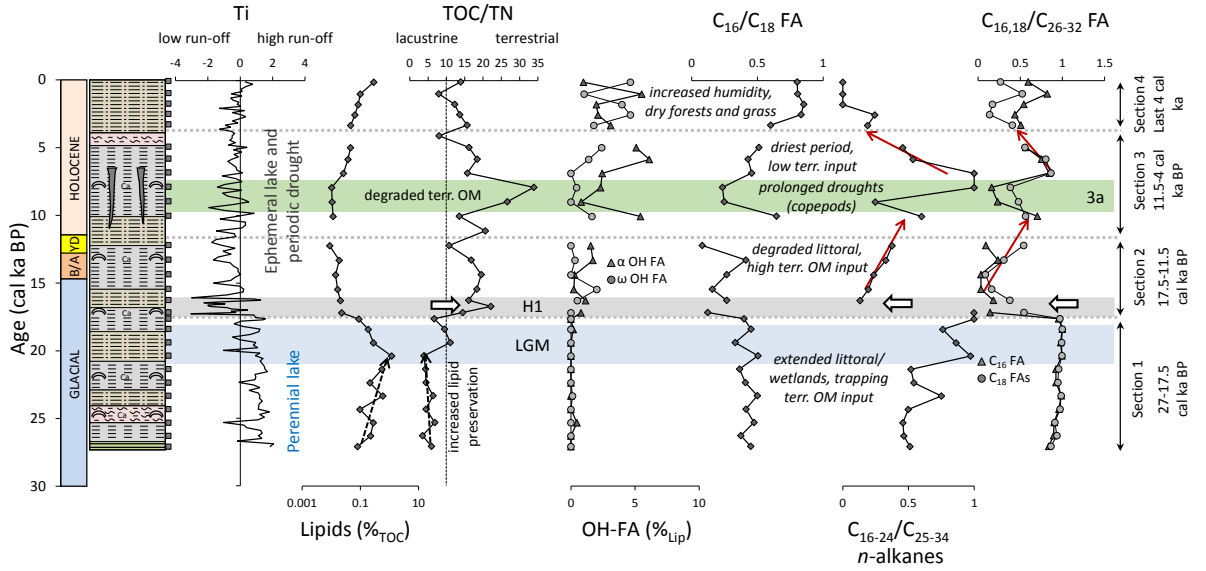

Figure 6 Comparison of proxy records of (inorganic) terrestrial runoff (Ti; Roy *et al*., 2015), lipid concentration relative to the total organic carbon ($\%_{TOC}$), total organic carbon to total nitrogen ratio (TOC/TN; Chavez-Lara *et al*., 2015), α and ω hydroxy acid (OH-FA) concentration ($\%_{Lip}$), C_{16}/C_{18} FA ratio, $C_{16\text{-}24}/C_{25\text{-}34}$ *n*-alkane ratio and $C_{16,18}/C_{26\text{-}32}$ FA ratio the Santiaguillo sedimentary profile, with the 4 Sections shown alongside basic interpretations. Note, e.g., the sharp changes in *n*-alkane and *n*-fatty acid distributions during Heinrich Stadial 1 (H1), the maximum TOC/TN ratios of Section 3a and the inversion of the relation between α- and ω-hydroxy acids in Section 4. H1 = Heinrich Stadial 1; LGM = last glacial maximum.

Section 1 (27 - 17.5 cal ka BP):

The early phase of this section corresponds to the later stages of the last glacial and it includes the last glacial maximum (LGM) lasting from ca. 21 to 18 cal ka BP. This section is characterised by aquatic (algal or bacterial) biomarkers (i.e. short-chain *n*-FAs) and relatively low abundances of terrestrial biomarkers (i.e. long-chain *n*-FAs). Collectively, all biomarker evidence is indicative of a system that sustained a perennial, highly productive lake with considerable input of bacterial biomass. There is hardly any evidence for input from the surrounding vegetation, which is surprising considering the fact that the basin received above average runoff during this interval (Roy *et al*., 2015), consistent with the existence of a perennial lake (Chávez-Lara *et al*., 2015). Plant remains from packrat middens indicate that the region was dominated by woodland species until 11.5 cal ka BP, including pinyon pines, juniper and shrub oak (Van Devender, 1990). We considered two hypotheses for explaining the lack of input from higher terrestrial vegetation. The first one is high in-lake productivity diluting the terrestrial inputs. However, the concentration of terrestrial biomarkers in this section is genuinely low (< 0.4 $\mu g/g_{sed}$,) and similar to the ranges observed in sections 2 and 3 and slightly lower than the biomarker concentration of section 4. The second and favoured hypothesis is that extended littoral zones trapped OM sourced from the catchment. The finding that, during the period from 27 to 17.5 cal ka BP, the Santiaguillo Basin harboured a year-round productive lake, with a stable water column and extended littoral zones contrasts a pollen record from the Chalco Basin in central Mexico (Fig. 1). There, the data suggests a desert climate during the last glacial (Lozano-García *et al*., 1993), implying a hydrological disconnect between the western Chihuahua Desert and central Mexico. Furthermore, the Community Earth System Model applied by Bhattacharya *et al*. (2017) for the LGM produces an East-West gradient in summer precipitation anomalies across central Mexico depending on ice-sheet extent and sea surface temperature, with the West experiencing drier conditions. Bhattacharya *et al*. (2017) hypothesize that local differences in the moist static energy budget are responsible for asymmetric extension of monsoonal convection over continental areas. It appears that regional hydrological boundaries and their lateral displacement over time cannot be sufficiently addressed based on the current slim

paleoenvironmental data base. In order to resolve the apparent patchiness in glacial moisture distribution across Mexico more evidence from paleoenvironmental archives is needed.

Section 2 (17.5 - 11.5 cal ka BP):

Section 2 corresponds to the deglaciation and it is characterised by much higher input from terrestrial vegetation compared to the glacial. More *Sphagnum* biomarkers (i.e. C_{23} *n*-alkane and methyl ketones) indicate the presence of ombrotrophic bogs in the surrounding catchment especially during 16- 11.7 cal ka BP. That would imply wetter conditions, but the Ti-based record suggests decreased runoff (Roy *et al*., 2015). Moreover, ostracod assemblages (Chávez-Lara *et al*., 2015) indicate that the lake level had dropped. Therefore, we suggest that these biomarker signatures reflect the exposure of wetland soils in the littoral zone and their erosion and transfer into the Santiaguillo Basin. During this interval, the vegetation of the Chihuahua Desert appears dominated by pinyon-juniper-oak woodland as suggested by packrat midden data from the northern (Van Devender, 1990) and southern parts of the desert (Van Devender and Burgess, 1985), with the latter records being closest to the Santiaguillo. While the long-chain *n*-FAs support an enhanced contribution of leaf waxes from a woodland environment to the Santiaguillo Basin, the increased proportions of *n*-alkanes (peaking at C_{31}), the supply of the C_{23} *n*-alkane (*Sphagnum*) and low amounts of lipids relative to TOC suggest a dominant supply of degraded OM mainly from a grassy (former) wetland area.

The onset of this section coincides with the Heinrich event 1 (H1: 17.2-16.3 cal ka BP; Figure 6). Interestingly, the paleoclimatic records from more northerly areas (e.g., the Gulf of California, Figure 1; McClymont *et al*., 2012) do not show a clear response to this cooling event, nor to the Younger Dryas (YD). In contrast, the records towards the south in central Mexico (i.e. Chalco Basin) indicate a distinct shift towards more humid conditions (16.5 ka, Lozano-García *et al*., 1993). At Santiaguillo, the H1 event is reflected by high-amplitude fluctuations in terrestrial runoff (Ti, Roy *et al*., 2015) and also abrupt shifts in both the amount and composition of the lipids supplied to the sediment. Specifically, the amount of lipids relative to the total organic carbon concentration dropped significantly to values below 0.1 $\%_{TOC}$ (minimum of 0.002 $\%_{TOC}$ at 16.7 cal ka BP), and compounds such as long-chain *n*-FAs, *n*-alkanes and, notably, 13-methoxyheneicosanoic acid increased sharply, with the latter reaching up to

41.7 $\%_{lipids}$ at 16.7 cal ka BP, indicating proportionally high input from bacterial biomass. Very similar conditions of high bacterial contributions (18.5 $\%_{lipids}$ of 13-methoxyheneicosanoic acid) were observed during the YD (12.2 cal ka BP). Therefore, compared to the glacial, the lake level in the Santiaguillo Basin appears to have dropped during the period of 17.5-11.5 cal ka BP or potentially fluctuated, causing degradation of former wetlands and associated supply of degraded OM.

Section 3 (11.5 - 4 cal ka BP):

This section corresponds to the early and mid-Holocene. In general, the biomarkers indicate reduced leaf wax inputs (long-chain *n*-FAs). Instead, contributions from woody plant tissues, as indicated by high C/N ratios but also consistent with bark and resin inputs (β-amyrin), appear to have increased. There is also evidence for significant inputs from bacterial biomass (short-chain *n*-FAs, α-C_{16} OH-FA) and aquatic plants (C_{21} *n*-alkane). The early phase of section 3 (11.5 – 9 cal ka BP) overlaps with expansion of modern grassland and provides evidence for increasing aridity beginning at 10 cal ka BP located towards the north, in the San Augustin Planes (Figure 1) (Sears and Clisby, 1956). This trend towards drier conditions appears to set in later, at about 9 cal ka BP in the Chihuahua Desert as seen in packrat midden records (Van Devender, 1990). In the Santiaguillo Basin, the input of terrestrial OM appears to maximise from 9 cal ka BP to 7.9 cal ka BP (subsection 3a) but it appears to be associated with predominantly woody material rather than leaf litter. The onset of this phase also coincides with a decrease in the abundance of ostracods (Chávez-Lara *et al*., 2015) and a contemporaneous increase in the abundance of copepods as implied by maximum relative amounts of the $C_{22:1}$ MUFA. This indicates a shift in the microfaunal community, probably as a response to a shallowing of the lake and the onset of seasonal droughts to which copepods tend to be more resistant than ostracods (Pillay and Perissinotto, 2009). The ostracod assemblage during this period (9-3.5 cal ka BP) also indicates the presence of an ephemeral lake with humid conditions only during summer months (Chávez-Lara *et al*., 2015). Enhanced aridity from about 9 cal ka BP is further documented by the disappearance of woodland plants, a decline of C_4 grasses and the establishment of desert scrubs in the Chihuahua Desert and, finally, expansion of desert grasslands at 8.3 ka (Van Devender, 1990; Buck and Monger, 1999).

Further aridification and extended periods of drought between 6.8 and 4.9 cal ka BP are indicated by the appearance of desiccation fissures at 6.2 cal ka BP (Fig. 6), lower than average terrestrial runoff as inferred from the Ti record (Roy *et al*., 2015; Fig. 6) and the disappearance of copepods as the source of the $C_{22:1}$ MUFA. During this phase, desert grassland in the northern part of the Chihuahua desert appeared more mesic than today (8.3-4.2 cal ka BP; Van Devender, 1990), while in the Sonora Desert winters were warmer than present (6.4-4.5 cal ka BP; McAuliffe and Van Devender, 1998). Towards the south, in central Mexico (Chalco Basin), the vegetation also declined (9-3 cal ka BP; Lozano-García *et al*., 1993). As aridity across the wider area generally increased and terrestrial OM inputs declined, relative contributions from algal and bacterial biomass to the Santiaguillo record increased (short-chain *n*-FAs, α-C_{16} OH-FA, C_{21} *n*-alkane), indicating at least short-lived occurrences of a water body during the summer season. Thus, from 11.5 to 4 cal ka BP (section 3), distinct phases of increasing aridity affecting the Santiaguillo ecosystem can be distinguished, in particular, the transition to a shallower, ephemeral lake with extended drought periods and associated microfaunal adaption between 9 and 7.9 cal ka BP (subsection 3a) and to even drier conditions supporting only a short-lived water body after 7.9 cal ka BP.

Section 4 (last 4 cal ka):

This uppermost section represents the late Holocene and it is marked by a change of sediment grain size from silty-clay to silty-sand. In terms of biomarkers, almost all higher plant biomarkers (long-chain ω-OH-FAs, *n*-alkanes, *n*-alcohols, sterols, and to a lesser degree, *n*-fatty acids) become more dominant. Modern subtropical dry forest vegetation, relying on seasonal moisture supply and with species rich in α-amyrin such as the *Burseraceae* family, might have been established at the beginning of this phase. This was apparently accompanied by the expansion of grasses growing among the open dry forest vegetation, as suggested by the bimodal *n*-alkane distribution with an enhanced proportion of the C_{31} *n*-alkane. At the same time, comparable vegetation change is reported from the north of the Chihuahua Desert, with more open habitats dominated by shrubs and succulents (3.9 cal ka BP; Van Devender and Worthington, 1977) and a recovery of the C_4 grasses (4 cal ka BP; Buck and Monger, 1999). The Sonora Desert experienced the establishment of modern desert scrub (4 cal ka BP; McAuliffe and Van

Devender, 1998). The expansion of the C_4 grasses, in this particular context, provides evidence for less severe aridity during the late Holocene summers as these grasses largely depend on summer precipitation (Throop *et al*., 2012; Báez *et al*., 2013). However, an increase in frequency and magnitude of the El Niño Southern Oscillation (ENSO) has been reconstructed over the last 4.2 cal ka (Moy *et al*., 2002; Conroy *et al*., 2008), which is typically associated with a general decrease in summer precipitation in the wider area (Magaña *et al*., 2003). However, during El Niño years, the north of Mexico also experiences more humid winters as a result of the increased sea surface temperatures in the NE Pacific (Ropelewski and Halpert, 1987) as well as an increased inflow of humid air masses from tropical Pacific cyclones in the autumn (Reyes and Mejia-Trejo, 1991; Rodgers *et al*., 2000; Englehart and Douglas, 2001; Jáuregui, 2003; Magaña *et al*., 2003; Larson *et al*., 2005), and both of these factors could have compensated for the drier summers. Thus, the reduced seasonal contrast in precipitation and the supply of moisture in autumn and winter during the late Holocene appeared to have supported an expansion of subtropical dry forests and grass lands that also represent the modern vegetation.

6. Conclusions

In this study, we used biomarker-based proxy data to reconstruct changes of the lacustrine and terrestrial environment of the Santiaguillo Basin in the western Chihuahua Desert (central-northern Mexico) over the past 27 cal ka. The lipid biomarker records reveal clearly distinguishable phases from a perennial lake with an extended littoral zone to an ephemeral lake and, ultimately, a dry basin. Furthermore, differences in the amount and composition of terrestrial biomarkers document the vegetation changes in the catchment, responding to the dynamics of the hydrological regime. Accordingly, during the last glacial period, the basin sustained a productive lake, with a stable water table and extended littoral zones that trapped most of the input from the surrounding terrestrial vegetation, which was probably dominated by woodland species. During the deglaciation, the lake level appears to have dropped and/or fluctuated, causing the degradation of the littoral wetlands and erosion of material from wetland soils into the lake. During the early Holocene, increasing aridity with extending periods of drought affected the aquatic ecosystem, turning the lake into a shallower, ephemeral lake and causing a shift in the macrofaunal community at 9 cal ka BP. After 7.9 cal ka BP,

the Santiaguillo Basin appears to have sustained only a short-lived water body and significant proportions of the deposited organic matter appear to have derived from bacterial biomass and the resin-rich bark litter from the surrounding desertscrubs. Over the last 4 cal ka, the distinctive modern vegetation of a subtropical dry forest along with grasses were established as a response to a reduced seasonal contrast in moisture supply, resulting from an increased frequency and magnitude of El Niño events.

Our study illustrates the great potential of biomarker applications for paleoenvironmental reconstructions that use depositional archives with poor preservation of pollen and other fossil particulate matter. It also confirms observations from paleoenvironmental studies in the wider area, i.e. the deserts of Northern Mexico and the Southwest of the USA. In particular, it supports and expands our understanding of the distinct climatic shift at about 4 cal ka BP that is related to the major reorganisation of atmospheric heat and moisture distribution observed across the Northern Hemisphere. Although the biomarker data from the Santiaguillo Basin provides evidence of changes in seasonality, other fundamental questions such as the source of precipitation, remain unresolved. We suggest that the determination of hydrogen isotope composition of terrestrial leaf-wax compounds (i.e., long-chain alkyl lipids), although not possible in this study due to the small sample size and low biomarker concentrations, could provide additional insight in future studies; such work, however, would have to recognise the complex changes in the sources of higher plant biomarkers as identified here.

Acknowledgements

This research was partly supported by CONACyT project (CB-237579). CMCL was awarded a scholarship from CONACyT (384524) for her doctoral study at the University of Bristol. Dr Ian Bull, Dr Megan Rohrssen, Alison Kuhl and Felipe Sales De Freitas provided technical assistance. Staff of Heroico Cuerpo de Bomberos and Protección Civil of Durango provided assistance and security to the expedition members during field visits and sampling. We are thankful to both reviewers and editor Prof. Xiaoping Yang for their critical comments and observations.

References

548 Ahlgren, G., Gustafsson, I.B. and Boberg, M., 1992. Fatty acid content and chemical composition of
549 freshwater microalgae. Journal of phycology, 28(1), pp.37-50.

550 Arts, M.T., Ackman, R.G. and Holub, B.J., 2001. "Essential fatty acids" in aquatic ecosystems: a crucial
551 link between diet and human health and evolution. Canadian Journal of Fisheries and Aquatic
552 Sciences, 58(1), pp.122-137.

553 Baas, M., Pancost, R., van Geel, B. and Damsté, J.S.S., 2000. A comparative study of lipids in
554 Sphagnum species. Organic Geochemistry, 31(6), pp.535-541.

555 Báez, S., Collins, S.L., Pockman, W.T., Johnson, J.E. and Small, E.E., 2013. Effects of experimental
556 rainfall manipulations on Chihuahuan Desert grassland and shrubland plant communities.
557 Oecologia, 172(4), pp.1117-1127.

558 Baker, E.A., and Martin, J.T., 1963. Cutin of plant cuticles. Nature, 199(4900), pp.1268-1270.

559 Barnathan, G., Bourgougnon, N. and Kornprobst, J.M., 1998. Methoxy fatty acids isolated from the red
560 alga, Schzymenia dubyi. Phytochemistry, 47(5), pp.761-765.

561 Bhattacharya, T., Tierney, J.E. and DiNezio, P., 2017. Glacial reduction of the North American
562 Monsoon via surface cooling and atmospheric ventilation. Geophysical Research Letters, 44,
563 pp.5113-5122.

564 Bliedtner, M., Schäfer, I.K., Zech, R., and von Suchodoletz, H., 2017. Leaf wax n-alkanes in modern
565 plants and topsoils from eastern Georgia (Caucasus) – implications for reconstructing regional
566 paleovegetation, Biogeosciences Discussions, doi:10.5194/bg-2017-277.

567 Bobbie, R.J. and White, D.C., 1980. Characterization of benthic microbial community structure by
568 high-resolution gas chromatography of fatty acid methyl esters. Applied and Environmental
569 Microbiology, 39(6), pp.1212-1222.

570 Brooks, P.W., Eglinton, G., Gaskell, S.J., McHugh, D.J., Maxwell, J.R. and Philp, R.P., 1976. Lipids
571 of recent sediments, Part I: straight-chain hydrocarbons and carboxylic acids of some temperate
572 lacustrine and sub-tropical lagoonal/tidal flat sediments. Chemical Geology, 18(1), pp.21-38.

573 Buck, B.J. and Monger, H.C., 1999. Stable isotopes and soil-geomorphology as indicators of Holocene
574 climate change, northern Chihuahuan Desert. Journal of Arid Environments, 43(4), pp.357-373.

575 Bush, R.T. and McInerney, F.A., 2013. Leaf wax n-alkane distributions in and across modern plants:
576 implications for paleoecology and chemotaxonomy. Geochimica et Cosmochimica Acta, 117,
577 pp.161-179.

578 Calvert, S.E., 2004. Beware intercepts: interpreting compositional ratios in multi-component sediments
579 and sedimentary rocks. Organic Geochemistry, 35(8), pp.981-987.

580 Chávez-Lara, C.M., Roy, P.D., Pérez, L., Sankar, G.M. and Lemus-Neri, V.H.L., 2015. Ostracode and
581 C/N based paleoecological record from Santiaguillo basin of subtropical Mexico over last 27 cal
582 kyr BP. Revista Mexicana de Ciencias Geológicas, 32(1), pp.1-10.

583 Cohen, Z. and Vonshak, A., 1991. Fatty acid composition of Spirulina and Spirulina-like cyanobacteria
584 in relation to their chemotaxonomy. Phytochemistry, 30(1), pp.205-206.

585 Conroy, J.L., Overpeck, J.T., Cole, J.E., Shanahan, T.M. and Steinitz-Kannan, M., 2008. Holocene
586 changes in eastern tropical Pacific climate inferred from a Galápagos lake sediment record.
587 Quaternary Science Reviews, 27(11), pp.1166-1180.

588 Cranwell, P.A., 1984. Lipid geochemistry of sediments from Upton Broad, a small productive lake.
589 Organic Geochemistry, 7(1), pp.25-37.

590 Cranwell, P.A., Eglinton, G. and Robinson, N., 1987. Lipids of aquatic organisms as potential
591 contributors to lacustrine sediments—II. Organic Geochemistry, 11(6), pp.513-527.

592 Cui, J., Huang, J. and Xie, S., 2008. Characterstics of seasonal variations of leaf n-alkanes and n-alkenes
593 in modern higher plants in Qingjiang, Hubei Province, China. Chinese Science Bulletin, 53(17),
594 pp.2659-2664.

595 Dastillung, M. and Corbet, B., 1978. La géochimie organique des sédiments marins profonds. I.
596 Hydrocarbures saturés et insatures des sédiments. Géochimie organique des sédiments marins
597 profonds, Orgon II, Atlantique. NE Brésil. CNRS, Paris, pp.293-323.

598 Debyser, Y., Pelet, R. and Dastillung, M., 1975. Géochimie organique des sédiments marins récents:
599 Mer Noire, Baltique, Atlantique (Mauritanie). Campos R, Goni J (eds) Advances in organic
600 geochemistry, pp.289-320.

601 Eglinton, G. and Hamilton, R.J., 1967. Leaf epicuticular waxes. Science, 156(3780), pp.1322-1335.

602 Englehart, P.J. and Douglas, A.V., 2001. The role of eastern North Pacific tropical storms in the rainfall
603 climatology of western Mexico. International Journal of Climatology, 21(11), pp.1357-1370.

604 Espinosa, D., Llorente, J. and Morrone, J.J., 2006. Historical biogeographical patterns of the species of
605 Bursera (Burseraceae) and their taxonomic implications. Journal of Biogeography, 33(11),
606 pp.1945-1958.

607 Ficken, K.J., Wooller, M.J., Swain, D.L., Street-Perrott, F.A. and Eglinton, G., 2002. Reconstruction of
608 a subalpine grass-dominated ecosystem, Lake Rutundu, Mount Kenya: a novel multi-proxy
609 approach. Palaeogeography, Palaeoclimatology, Palaeoecology, 177(1), pp.137-149.

610 Freudenthal, T., Wagner, T., Wenzhöfer, F., Zabel, M. and Wefer, G., 2001. Early diagenesis of organic
611 matter from sediments of the eastern subtropical Atlantic: evidence from stable nitrogen and
612 carbon isotopes. Geochimica et Cosmochimica Acta, 65(11), pp.1795-1808.

613 Goad L.J. and Goodwin T.W., 1972. The biosynthesis of plant sterols. Progress in Phytochemistry, 3,
614 pp.113-198.

615 Grimalt, J. and Albaigés, J., 1987. Sources and occurrence of C12-C22 n-alkane distributions with even
616 carbon-number preference in sedimentary environments. Geochimica et Cosmochimica Acta,
617 51(6), pp.1379-1384.

618 Grimalt, J., Albaigés, J., Alexander, G. and Hazai, I., 1986. Predominance of even carbon-numbered n-
619 alkanes in coal seam samples of Nograd Basin (Hungary). Naturwissenschaften, 73(12), pp.729-
620 731.

621 Grogan, D.W. and Cronan, J.E., 1997. Cyclopropane ring formation in membrane lipids of bacteria.
622 Microbiology and Molecular Biology Reviews, 61(4), pp.429-441.

Han, J. and Calvin, M., 1969. Hydrocarbon distribution of algae and bacteria, and microbiological activity in sediments. Proceedings of the National Academy of Sciences, 64(2), pp.436-443.

Han, J., McCarthy, E.D., Van Hoeven, W., Calvin, M. and Bradley, W.H., 1968. Organic geochemical studies, II. A preliminary report on the distribution of aliphatic hydrocarbons in algae, in bacteria, and in a recent lake sediment. Proceedings of the National Academy of Sciences, 59(1), pp.29-33.

Hernández-Vázquez, L., Palazon, J. and Navarro-Ocaña, A., 2012. The pentacyclic triterpenes α-, β-amyrins: a review of sources and biological activities. Phytochemicals-A Global Perspective of Their Role in Nutrition and Health, 23, pp.487-502.

Holmgren, C.A., Betancourt, J.L. and Rylander, K.A., 2006. A 36,000-yr vegetation history from the Peloncillo Mountains, southeastern Arizona, USA. Palaeogeography, Palaeoclimatology, Palaeoecology, 240(3), pp.405-422.

Holmgren, C.A., Norris, J. and Betancourt, J.L., 2007. Inferences about winter temperatures and summer rains from the late Quaternary record of C4 perennial grasses and C3 desert shrubs in the northern Chihuahuan Desert. Journal of Quaternary Science, 22(2), pp.141-161.

Holmgren, C.A., Penalba, M.C., Rylander, K.A. and Betancourt, J.L., 2003. A 16,000 14 C yr BP packrat midden series from the USA–Mexico Borderlands. Quaternary Research, 60(3), pp.319-329.

Holtvoeth, J., Rushworth, D., Copsey, H., Imeri, A., Cara, M., Vogel, H., Wagner, T. and Wolff, G.A., 2016. Improved end-member characterisation of modern organic matter pools in the Ohrid Basin (Albania, Macedonia) and evaluation of new palaeoenvironmental proxies. Biogeosciences, 13(3), pp.795-816.

Jáuregui, E., 2003. Climatology of landfalling hurricanes and tropical storms in Mexico. Atmósfera, 16(4), pp.193-204.

647 Kattner, G., Gercken, G. and Hammer, K.D., 1983. Development of lipids during a spring plankton
648 bloom in the northern North Sea: II. Dissolved lipids and fatty acids. Marine chemistry, 14(2),
649 pp.163-173.

650 Kerger, B.D., Nichols, P.D., Antworth, C.P., Sand, W., Bock, E., Cox, J.C., Langworthy, T.A. and
651 White, D.C., 1986. Signature fatty acids in the polar lipids of acid-producing Thiobacillus spp.:
652 methoxy, cyclopropyl, alpha-hydroxy-cyclopropyl and branched and normal monoenoic fatty
653 acids. FEMS Microbiology Ecology, 2(2), pp.67-77.

654 Kolattukudy, P. E., 1981. Structure, biosynthesis, and biodegredation of cutin and suberin. Annual
655 Review Plant Physiolgy, 32, pp.539-67.

656 Kunst, L. and Samuels, A.L., 2003. Biosynthesis and secretion of plant cuticular wax. Progress in lipid
657 research, 42(1), pp.51-80.

658 Lachniet, M.S., Asmerom, Y., Bernal, J.P., Polyak, V.J. and Vazquez-Selem, L., 2013. Orbital pacing
659 and ocean circulation-induced collapses of the Mesoamerican monsoon over the past 22,000 y.
660 Proceedings of the National Academy of Sciences, 110(23), pp.9255-9260.

661 Larson, J., Zhou, Y. and Higgins, R.W., 2005. Characteristics of landfalling tropical cyclones in the
662 United States and Mexico: Climatology and interannual variability. Journal of Climate, 18(8),
663 pp.1247-1262.

664 Lozano-García, M.S., Ortega-Guerrero, B. and Sosa-Nájera, S., 2002. Mid-to late-Wisconsin pollen
665 record of San Felipe basin, Baja California. Quaternary Research, 58(1), pp.84-92.

666 Lozano-García, M.S., Ortega-Guerrero, B., Caballero-Miranda, M. and Urrutia-Fucugauchi, J., 1993.
667 Late Pleistocene and Holocene paleoenvironments of Chalco Lake, central Mexico. Quaternary
668 Research, 40(3), pp.332-342.

669 Maffei, M., 1996. Chemotaxonomic significance of leaf wax alkanes in the Gramineae. Biochemical
670 systematics and ecology, 24(1), pp.53-64.

671 Magaña, V.O., Vázquez, J.L., Pérez, J.L. and Pérez, J.B., 2003. Impact of El Niño on precipitation in
672 Mexico. Geofísica internacional, 42(3), pp.313-330.

673 Matsuda, H. and Koyama, T., 1977. Early diagenesis of fatty acids in lacustrine sediments—II. A
674 statistical approach to changes in fatty acid composition from recent sediments and some source
675 materials. Geochimica et Cosmochimica Acta, 41(12), pp.1825-1834.

676 McAuliffe, J.R., and Van Devender, T.R., 1998. A 22,000-year record of vegetation change in the north-
677 central Sonoran Desert. Palaeogeography, Palaeoclimatology, Palaeoecology, 141(3), pp. 253-
678 275.

679 McClymont, E.L., Ganeshram, R.S., Pichevin, L.E., Talbot, H.M., Dongen, B.E., Thunell, R.C.,
680 Haywood, A.M., Singarayer, J.S. and Valdes, P.J., 2012. Sea-surface temperature records of
681 Termination 1 in the Gulf of California: Challenges for seasonal and interannual analogues of
682 tropical Pacific climate change. Paleoceanography, 27(2).

683 Metcalfe, S., Say, A., Black, S., McCulloch, R. and O'Hara, S., 2002. Wet conditions during the last
684 glaciation in the Chihuahuan Desert, Alta Babicora Basin, Mexico. Quaternary Research, 57(1),
685 pp.91-101.

686 Metcalfe, S.E., Barron, J.A., Davies, S.J., 2015. The Holocene history of the North American Monsoon:
687 'known knowns' and 'known unknowns' in understanding its spatial and temporal complexity.
688 Quaternary Science Reviews, 120, pp.1-27.

689 Meyers, P.A. and Benson, L.V., 1988. Sedimentary biomarker and isotopic indicators of the
690 paleoclimatic history of the Walker Lake basin, western Nevada. Organic Geochemistry, 13,
691 pp.807-813.

692 Meyers, P.A. and Ishiwatari, R., 1993. Lacustrine organic geochemistry - an overview of indicators of
693 organic matter sources and diagenesis in lake sediments. Organic geochemistry, 20(7), pp.867-
694 900.

695 Meyers, P.A., 2003. Applications of organic geochemistry to paleolimnological reconstructions: a
696 summary of examples from the Laurentian Great Lakes. Organic geochemistry, 34(2), pp.261-
697 289.

698 Meyers, P.A., Leenheer, M.J., Eaoie, B.J. and Maule, S.J., 1984. Organic geochemistry of suspended
699 and settling particulate matter in Lake Michigan. Geochimica et Cosmochimica Acta, 48(3),
700 pp.443-452.

701 Moy, C.M., Seltzer, G.O., Rodbell, D.T. and Anderson, D.M., 2002. Variability of El Niño/Southern
702 Oscillation activity at millennial timescales during the Holocene epoch. Nature, 420(6912),
703 pp.162-165.

704 Nieto-Samaniego, Á.F., Barajas-Gea, C.I., Gómez-González, J.M., Rojas, A., Alaniz-Álvarez, S.A. and
705 Xu, S., 2012. Geología, evolución estructural (Eoceno al actual) y eventos sísmicos del Graben
706 de Santiaguillo, Durango, México. Revista mexicana de ciencias geológicas, 29(1), pp.115-130.

707 Nott, C.J., Xie, S., Avsejs, L.A., Maddy, D., Chambers, F.M. and Evershed, R.P., 2000. n-Alkane
708 distributions in ombrotrophic mires as indicators of vegetation change related to climatic
709 variation. Organic Geochemistry, 31(2), pp.231-235.

710 Orgambide, G.G., Reusch, R.N. and Dazzo, F.B., 1993. Methoxylated fatty acids reported in Rhizobium
711 isolates arise from chemical alterations of common fatty acids upon acid-catalyzed
712 transesterification procedures. Journal of bacteriology, 175(15), pp.4922-4926.

713 Oster, J.L., Ibarra, D.E., Winnick, M.J. and Maher, K., 2015. Steering of westerly storms over western
714 North America at the Last Glacial Maximum. Nature Geoscience, 8(3), p.201.

715 Palacios-Fest, M.R., Carreño, A.L., Ortega-Ramírez, J.R. and Alvarado-Valdéz, G., 2002. A
716 paleoenvironmental reconstruction of Laguna Babícora, Chihuahua, Mexico based on ostracode
717 paleoecology and trace element shell chemistry. Journal of Paleolimnology, 27(2), pp.185-206.

718 Perry, G.J., Volkman, J.K., Johns, R.B. and Bavor, H.J., 1979. Fatty acids of bacterial origin in
719 contemporary marine sediments. Geochimica et Cosmochimica Acta, 43(11), pp.1715-1725.

720 Pillay, D. and Perissinotto, R., 2009. Community structure of epibenthic meiofauna in the St. Lucia
721 Estuarine Lake (South Africa) during a drought phase. Estuarine, Coastal and Shelf Science,
722 81(1), pp.94-104.

723 Poger, D. and Mark, A.E., 2015. A ring to rule them all: the effect of cyclopropane Fatty acids on the
724 fluidity of lipid bilayers. The journal of physical chemistry B, 119(17), pp.5487-5495.

725 Porter, D.M., 1974. The Burseraceae in North America north of Mexico. Madrono, 22(5), pp.273-276.

726 Quiroz-Jimenez, J.D., Roy, P.D., Lozano-Santacruz, R. and Giron-García, P., 2017. Hydrological
727 responses of the Chihuahua Desert of Mexico to possible Heinrich Stadials. Journal of South
728 American Earth Sciences, 73, pp.1-9.

729 Ramirez, M.E., Nuñez, J.D., Ocampo, E.H., Matula, C.V., Suzuki, M., Hashimoto, T. and Cledón, M.,
730 2012. Schizymenia dubyi (Rhodophyta, Schizymeniaceae), a new introduced species in
731 Argentina. New Zealand Journal of Botany, 50(1), pp.51-58.

732 Reimer, P.J., Bard, E., Bayliss, A., Beck, J.W., Blackwell, P.G., Ramsey, C.B., Buck, C.E., Cheng, H.,
733 Edwards, R.L., Friedrich, M. and Grootes, P.M., 2013. IntCal13 and Marine13 radiocarbon age
734 calibration curves 0–50,000 years cal BP. Radiocarbon, 55(4), pp.1869-1887.

735 Reyes, S. and Mejía-Trejo, A., 1991. Tropical perturbations in the Eastern Pacific and the Precipitation
736 field over North-Western Mexico in relation to the ENSO phenomenon. International Journal of
737 Climatology, 11(5), pp.515-528.

738 Řezanka, T. and Sigler, K., 2009. Odd-numbered very-long-chain fatty acids from the microbial, animal
739 and plant kingdoms. Progress in lipid research, 48(3), pp.206-238.

740 Rodgers, E.B., Adler, R.F. and Pierce, H.F., 2000. Contribution of tropical cyclones to the North Pacific
741 climatological rainfall as observed from satellites. Journal of Applied Meteorology, 39(10),
742 pp.1658-1678.

743 Rommerskirchen, F., Plader, A., Eglinton, G., Chikaraishi, Y. and Rullkötter, J., 2006.
744 Chemotaxonomic significance of distribution and stable carbon isotopic composition of long-
745 chain alkanes and alkan-1-ols in C4 grass waxes. Organic Geochemistry, 37(10), pp.1303-1332.

746 Ropelewski, C.F. and Halpert, M.S., 1987. Global and regional scale precipitation patterns associated
747 with the El Niño/Southern Oscillation. Monthly weather review, 115(8), pp.1606-1626.

748 Roy, P.D., Caballero, M., Lozano, S., Morton, O., Lozano, R., Jonathan, M.P., Sánchez, J.L. and
749 Macías, M.C., 2012. Provenance of sediments deposited at paleolake San Felipe, western Sonora
750 Desert: Implications to regimes of summer and winter precipitation during last 50 cal kyr BP.
751 Journal of Arid Environments, 81, pp.47-58.

752 Roy, P.D., Chávez-Lara, C.M., Beramendi-Orosco, L.E., Sánchez-Zavala, J.L., Muthu-Sankar, G.,
753 Lozano-Santacruz, R., Quiroz-Jimenez, J.D. and López-Balbiaux, N., 2015. Paleohydrology of
754 the Santiaguillo Basin (Mexico) since late last glacial and climate variation in southern part of
755 western subtropical North America. Quaternary Research, 84(3), pp.335-347.

756 Roy, P.D., Quiroz-Jimenez, J.D., Pérez-Cruz, L.L., Lozano-García, S., Metcalfe, S.E., Lozano-
757 Santacruz, R., López-Balbiaux, N., Sánchez-Zavala, J.L. and Romero, F.M., 2013. Late
758 Quaternary paleohydrological conditions in the drylands of northern Mexico: a summer
759 precipitation proxy record of the last 80 cal ka BP. Quaternary Science Reviews, 78, pp.342-354.

760 Roy, P.D., Rivero-Navarrete, A., Sánchez-Zavala, J.L., Beramendi-Orosco, L.E., Muthu-Sankar, G. and
761 Lozano-Santacruz, R., 2016. Atlantic Ocean modulated hydroclimate of the subtropical
762 northeastern Mexico since the last glacial maximum and comparison with the southern US. Earth
763 and Planetary Science Letters, 434, pp.141-150.

764 Samuels, L., Kunst, L. and Jetter, R., 2008. Sealing plant surfaces: cuticular wax formation by epidermal
765 cells. Annual review of plant biology, 59, pp.683-707.

766 Sears, P.B. and Clisby, K.H., 1956. San Agustin Planes-Pleistocene climatic changes. Science, 124,
767 pp.537-539.

768 Servicio Meteorológico Nacional (SMN), México. Estación 10137 Guatimape (DGE) (24°48'25" N.,
769 104°55'19" W., 1,974.0 msnm). Normales Climatológicas 1981-2010.
770 <http://smn.cna.gob.mx/tools/RESOURCES/Normales8110/NORMAL10137.TXT>, August,
771 2017.

772 Singh, S.C., Sinha, R.P. and Hader, D.P., 2002. Role of lipids and fatty acids in stress tolerance in
773 cyanobacteria. Acta protozoologica, 41(4), pp.297-308.

774 Throop, H.L., Reichmann, L.G., Sala, O.E. and Archer, S.R., 2012. Response of dominant grass and
775 shrub species to water manipulation: an ecophysiological basis for shrub invasion in a
776 Chihuahuan Desert grassland. Oecologia, 169(2), pp.373-383.

777 van Bree, L.G., Rijpstra, W.I.C., Al-Dhabi, N.A., Verschuren, D., Damsté, J.S. and de Leeuw, J.W.,
778 2016. Des-A-lupane in an East African lake sedimentary record as a new proxy for the stable
779 carbon isotopic composition of C3 plants. Organic Geochemistry, 101, pp.132-139.

780 Van Devender, T.R. and Burgess, T.L., 1985. Late Pleistocene woodlands in the Bolson de Mapimi: A
781 refugium for the Chihuahuan Desert Biota? Quaternary Research, 24(3), pp.346-353.

782 Van Devender, T.R., 1990. Late quaternary vegetation and climate of the Chihuahuan Desert, United
783 States and Mexico (pp. 104-133). Tucson, AZ: University of Arizona Press.

784 Van Devender, T.R., and Worthington, R.D., 1977. The herpetofauna of Howell's Ridge Cave and the
785 paleoecology of the northwestern Chihuahuan Desert. In Transactions of the Symposium on the
786 Biological Resources of the Chihuahuan Desert Region, United States and Mexico: National Park
787 Service Transactions and Proceedings, 3, pp.85-106.

788 Volkman, J.K., 1986. A review of sterol markers for marine and terrigenous organic matter. Organic
789 Geochemistry, 9(2), pp.83-99.

790 Volkman, J.K., 2005. Sterols and other triterpenoids: source specificity and evolution of biosynthetic
791 pathways. Organic geochemistry, 36(2), pp.139-159.

792 Walker, M.J., Berkelhammer, M., Björck, S., Cwynar, L.C., Fisher, D.A., Long, A.J., Lowe, J.J.,
793 Newnham, R.M., Rasmussen, S.O. and Weiss, H., 2012. Formal subdivision of the Holocene
794 Series/Epoch: a Discussion Paper by a Working Group of INTIMATE (Integration of ice-core,
795 marine and terrestrial records) and the Subcommission on Quaternary Stratigraphy (International
796 Commission on Stratigraphy). Journal of Quaternary Science, 27(7), pp.649-659.

797 Wood, A.P. and Kelly, D.P., 1991. Isolation and characterisation of Thiobacillus halophilus sp. nov., a
798 sulphur-oxidising autotrophic eubacterium from a Western Australian hypersaline lake. Archives
799 of microbiology, 156(4), pp.277-280.

800 Yano, I., Furukawa, Y. and Kusunose, M., 1971. Fatty-Acid Composition of Arthrobacter simplex
801 Grown on Hydrocarbons. The FEBS Journal, 23(2), pp.220-228.